Monte Carlo Investigation of Particle Properties Affecting TPB Formation and Conductivity in Composite Solid Oxide Fuel Cell Electrode-Electrolyte Interfaces

Andrew Martinez
e-mail: asm@nfcrc.uci.edu

Jacob Brouwer
e-mail: jb@nfcrc.uci.edu

National Fuel Cell Research Center,
University of California-Irvine,
Irvine, CA 92697-3550

A previously developed microstructure model of a solid oxide fuel cell (SOFC) electrode-electrolyte interface has been applied to study the impacts of particle properties on these interfaces through the use of a Monte Carlo simulation method. Previous findings that have demonstrated the need to account for gaseous phase percolation have been confirmed through the current investigation. In particular, the effects of three-phase percolation critically affect the dependence of TPB formation and electrode conductivity on (1) conducting phase particle size distributions, (2) electronic:ionic conduction phase contrast, and (3) the amount of mixed electronic-ionic conductor (MEIC) included in the electrode. In particular, the role of differing percolation effectiveness between electronic and ionic phases has been shown to counteract and influence the role of the phase contrast. Porosity, however, has been found to not be a significant factor for active TPB formation in the range studied, but does not obviate the need for modeling the gas phase. In addition, the current work has investigated the inconsistencies in experimental literature results concerning the optimal particle size distribution. It has been found that utilizing smaller particles with a narrow size distribution is the preferable situation for electrode-electrolyte interface manufacturing. These findings stress the property-function relationships of fuel cell electrode materials. [DOI: 10.1115/1.4003781]

Keywords: solid oxide fuel cell; electrode-electrolyte interface; Monte Carlo model; percolation

1 Introduction

The ability to form triple phase boundaries (TPB) within the electrode-electrolyte interfaces of fuel cells, and in particular composite solid oxide fuel cells (SOFCs), has long been accepted as critical to the manufacture of high-performance fuel cells. It has therefore naturally been of interest within the field to understand how to best manufacture and design cells such that the formation of these electrochemically active regions within the electrodes is optimized. Previous modeling efforts developed to study the percolation-related aspects of manufacturing these structures have typically focused upon and accentuated the roles of the electron- and ion-conducting material phases, especially when the major consideration is the overall conductivity of the electrode rather than the formation of the TPBs themselves. Common practices, as followed by researchers such as Sunde and Costamagna et al., have therefore modeled the electrode structure as comprised of two phases and followed with assumptions that the materials are themselves porous enough (implying porosity only on a dimensional scale smaller than an individual conducting particle) to allow gaseous diffusion without any limitations throughout the electrode [1,2]. However, it has been shown through the use of a similarly formulated Monte Carlo model, which includes gas phase percolation, that the development of large pore structures in the electrode plays a critical role in the formation of the TPBs, especially as it interacts with the electronic phase [3,4]. In spite of overlooking the gaseous phase, the prior modeling efforts have made useful observations of the basic percolation properties and identified key factors in the optimization of electrode microstructure. Composition has been repeatedly reported to have primary importance by Deseure et al., Sunde et al., and others [1–7]. In addition, the impacts of particle-specific properties, such as the relative conductivities of the ionic and electronic phases and particle size distribution, have been investigated by Schneider et al., Virkar et al., and others [5–8]. These features of the particles have been consistently found to express themselves in the overall performance of the electrode and electrode-electrolyte interface.

All of these previous studies have incorporated a model that studies the electrode structure through a Monte Carlo method that analyzes a given number of representative electrode structures. The use of Monte Carlo methods within the literature has been motivated by the nature of the methods that are most commonly utilized to manufacture these electrode-electrolyte interfaces. These methods include advanced procedures such as aerosol-assisted vapor deposition, magnetron sputtering, and flame and plasma spraying as well as more traditional methods such as tape casting and calendaring and screen printing [9–16]. These are typically intermixed with various stages of ball milling, randomized particle mixing, particle sizing and preparation, and heat treatments, including calcining and sintering.

Common to all of these processes is the inability to engineer or directly control and/or predict the details of the final microstructure of the electrodes, especially the relative positioning and interconnection of different phases of material in the electrode-electrolyte interface. For an SOFC, this typically includes at least the three different phases mentioned above (ionic, electronic, gas), all of which must have percolating, interconnected structures in order for the electrode to function as desired. In addition, specialized material

Contributed by the Advanced Energy Systems Division of ASME for publication in the JOURNAL OF FUEL CELL SCIENCE AND TECHNOLOGY. Manuscript received January 3, 2011; final manuscript received January 27, 2011; published online June 29, 2011. Editor: Nigel M. Sammes.

Copyright © 2011 by ASME

Downloaded From: http://fuelcellscience.asmedigitalcollection.asme.org/ on 02/06/2015 Terms of Use: http://asme.org/terms

phases such as mixed electronic-ionic conductors (MEIC) may be included in an effort to enhance the performance of the cell by increasing TPB line length and/or reduction of ohmic resistance. Finally, surfactants, pore formers, and binders are often included in the original electrode composition in order to support the manufacturing processes, although these materials are not typically present in the final structure due to removal that occurs during the various manufacturing steps. The intermixing of these various phases, even those which are removed during processing, has marked impacts on the final microstructure of the electrode, and therefore affects the overall performance.

Experimental investigations of the performance of SOFC electrodes have provided insight into the optimal material properties and parameters for their manufacture. Investigations have focused on a wide range of material sets, including the traditional nickel-yttria-stabilized zirconia (YSZ) electrode as well as gadolina-doped ceria (CGO) and strontium-doped lanthanum manganite (LSM). These works have highlighted the pertinence of processing steps as well as individual particle properties to performance. In particular, the temperatures of calcining and sintering processing steps have been repeatedly found to play a vital role through the works of Juhl et al. and others [17–20], as has the overall thickness of the electrode by Sasaki et al. and Juhl et al. [17,18]. In addition, particle-specific properties have been identified as particularly pertinent. Dusastre and Kilner as well as Ostergard et al. have demonstrated the usefulness of MEICs, given the specialized function these materials are able to provide [20,21]. Particle size distribution has also been noted as especially important, although there has been some disagreement as to the optimal conditions in this regard. Sasaki et al. have reported a narrow size distribution to be the most desirable, while researchers such as van Hueveln et al. and Ostergard et al. have indicated a preference for broader, or even bimodal particle size distributions [18,19,21]. These insights, though sometimes contested and unresolved, have formed the basis of knowledge for the practical optimization of SOFC electrode-electrolyte interface construction.

However, these investigations typically have not developed an understanding of the mechanisms responsible for their observations. Indeed, this has been one of the motivating factors for modeling the structure-function and property-function relationships in fuel cell electrodes. Although some of these factors have been investigated with the previously developed models, the inclusion of the gas phase has already been noted to be of particular importance in the electrode structure and performance. Thus, it could be expected that some of the previous observations, insights and understanding could be altered by consideration of this gas phase percolation through the electrode.

Previous investigations by the authors [3,4] have explored the fundamentals of these TPB-forming interactions with the inclusion of the gas phase structure as well as novel considerations such as the structure of the current collector and its effect on percolation and conductivity in the electrode. In order to complement the findings of this previous work, the current work attempts to provide more detailed information about these processes by investigating the ways in which they depend upon the properties of the materials included in electrode manufacture. These particle- and material-specific properties are investigated in order to make the connection between properties and their functions in the electrode structure.

2 Model Description

A model that simulates the structure of an SOFC electrode-electrolyte interface was developed and utilized to explore the fundamentals of the requirements established by percolation of multiple (three) phases in a geometry that is typical of an SOFC electrode-electrolyte interface. The model was used to study how three-phase percolation in representative geometries influences the formation of TPBs [3] and the overall conductivity of the electrode [4]. Although the details of the model have been discussed previously, certain capabilities of the model were not fully utilized in the previous studies, particularly those features imparted by the

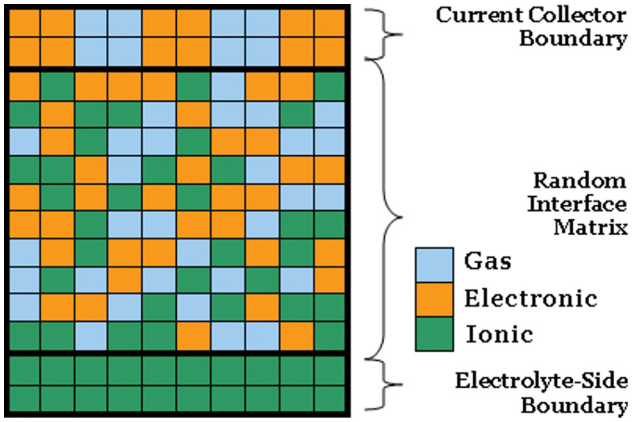

Fig. 1 Representative monodisperse electrode-electrolyte interface; blue denotes gas, orange denotes electron conducting phase, and green denotes ion conducting phase

properties of the specific materials used to build the electrode. This investigation focuses upon these particle-based properties and their contributions to electrode performance within the context of the simulation results previously presented. The full details of the electrode simulation software have been discussed [3,4], but a brief summary description is provided below.

The model is based on the formation of a digitized, two-dimensional representation of the electrode-electrolyte interface, as shown in Fig. 1. The structure of this electrode is formed by random assignment of particles within the Cartesian grid defined as the overall simulation geometry. Through an iterative process, the software chooses a location, particle type, particle size, and orientation; checks for the required space for the particle at the chosen location; checks that placement of the particle will not violate the composition requirements (some error is allowed in particle size distribution, as discussed below), and if all checks return positive, allows the particle to be placed at the chosen location. If the particle violates any of the checks, then the software chooses a new particle, sometimes with some of the properties of the previous particle (this is merely part of the optimization of the code—it is not always necessary to choose a completely new set of parameters for the particle). If, after a tunable number of attempts, the particle cannot be placed, a particle of the same type, but with a size equal to a single cell in the grid, is chosen and placed in the electrode since this result is always positive.

This process is repeated until the entirety of the electrode geometry is filled with particles of the types defined by the user, in the ratios defined by the user. The user inputs are therefore the selection of the particle types to be included in the electrode, each of those particle types' volume fractions and particle size distributions, the conductivities of appropriate particle types, the porosity of the electrode, the size of the grid to be utilized in the simulation, and the number of simulations to be run. Although it would be ideal, it is not always possible to utilize any given set of particle size distributions in combination with a set of particle type volume fractions to fill the electrode and still develop a sufficient number of independent electrode structures for statistical significance. Thus, the model was made able to handle the possibility of including some error between the user settings and the realized electrode structures. In practice, control of the composition is more readily available and characterized than control of the particle size distribution for any given material. Therefore, the simulation allows for error in the particle size distribution, in particular, to preserve the composition defined by the user inputs. It should be noted that the error was allowed to be both positive and negative in all particle sizes to avoid bias.

The particle sizes and orientation options are presented in Fig. 2. The shaded cell in each particle size illustration is the cell utilized as the "seed" location, which was used as the basis cell

Downloaded From: http://fuelcellscience.asmedigitalcollection.asme.org/ on 02/06/2015 Terms of Use: http://asme.org/terms

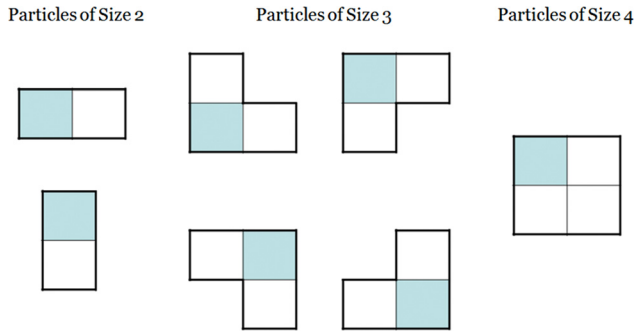

Fig. 2 Particle size definitions with seed location indicated by shaded cell

for checking if the remaining cells required for placement of the particle are free in the electrode structure's grid. In addition to the particles shown, a particle of size 1, a single cell, was also utilized, and the single cell was then of course also the seed location. Seven different particle size and shape distributions were studied; six of these are shown in Fig. 3, and the final distribution was both electronic and ionic particles consisting entirely of particles of size 1, termed the monodisperse case. These specific particle distributions were chosen for a variety of reasons. Foremost, they were chosen to verify whether or not particle size distribution has any effect at all, and so a variety of distributions was desirable for this determination. In addition, it was of interest to study the disagreement in results between Sasaki et al. and others. Finally, it has been noticed that electronic and ionic phases do not behave equivalently with respect to percolation of the phases and the effect this has on performance [3,4]. Thus, distributions that reflect contrasts between these two phases are desirable in this investigation.

Subsequent to the formation of the randomized electrode structure, the boundary conditions at the current collector and the electrolyte were appended to the electrode. On the electrolyte side, the boundary consisted entirely of ionically conducting particles, in order to simulate the dense electrolyte structure which is required for SOFC operation. On the current collector side, the boundary condition was defined by the user. The full spectrum of boundary conditions defined for use by the model has been presented [3]; however, only select versions of these combined gas and electronic phase boundary conditions were utilized in this investigation, and will be discussed below, as appropriate. The full set of current collectors used with this and previous investigations of the

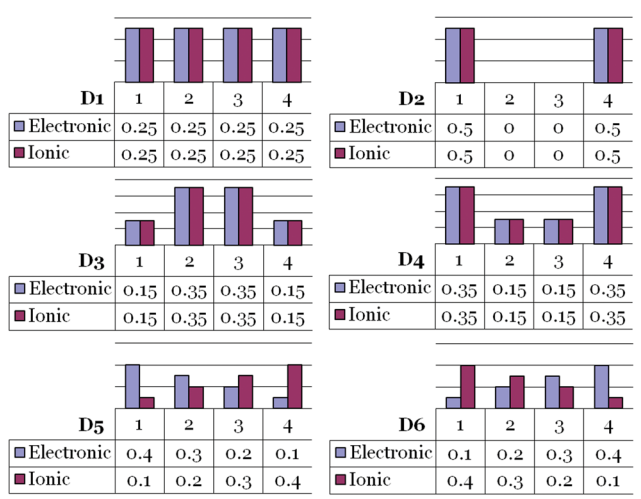

Fig. 3 Particle size distributions utilized in simulations

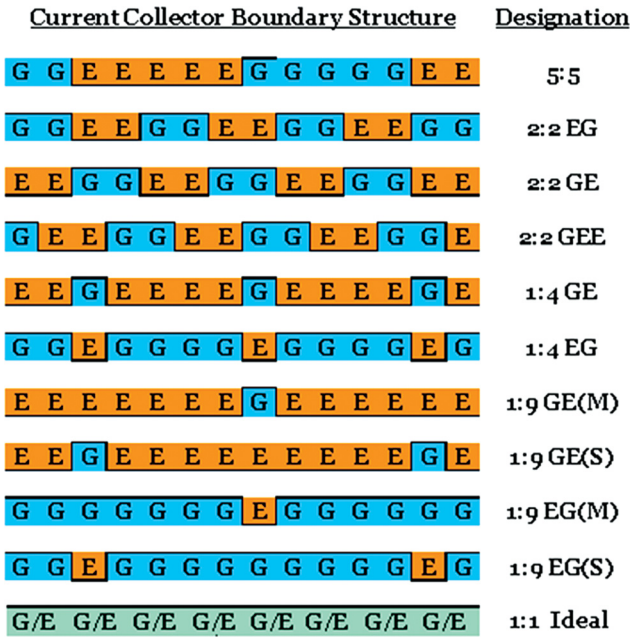

Fig. 4 Current collector boundary conditions

model is depicted in Fig. 4. With the inclusion of these gas-electronic boundary conditions, the electrode formation portion of the model was completed. Following this portion, the model then executed the electrode analysis routine for each of the instances considered in the full Monte Carlo simulation.

The first step in this analysis was the identification of TPBs, for which there were two classifications. These have been labeled as active and potential TPBs. Potential TPBs are defined merely by the adjacency of the three required phases-electronic, ionic, and gas phase. Active TPBs are defined by the additional requirement that a full percolating path must be present for each phase between the particles at the TPB and the appropriate boundary, i.e., electrolyte for the ionic phase and current collector for the electronic and gas phases. In addition, the definition for the adjacency of the gas phase was adjustable to include the effects of surface exchange and transport phenomena, previously referred to as sorbate transport [3], as described by Adler [22]. The model accounted for these processes by allowing a gas phase particle to contribute to forming a TPB even if it was one particle removed from the interface between an electronic and ionic phase particle. This allowed TPBs to be more readily formed anywhere in the electrode, and extended the effective active area of TPBs, similar to what occurs in SOFC cathodes. Simulations were therefore studied both with and without surface exchange and transport phenomena enabled in order to investigate the pervasiveness of the impacts of these processes on the performance of SOFC electrodes.

The second portion of analysis involved the calculation of the overall conductivity of the composite electrode. As such, the conductivity calculated in this step represents an effective conductivity attributed to both the ionic and electronic conduction pathways through the electrode. In order to perform the calculation, the full percolating network connected to the TPB for both electronic and ionic phases was converted to a network of conducting elements, where conducting elements were placed along each edge of every particle belonging to the network. It should be noted that although the model utilizes the edges of the particles as the basis for the conducting network's geometry, the model is not a surface conduction model; rather, bulk conductivities of all materials were utilized in all simulations. The use of conduction paths along edges simply allows the model to account for the possibility of multiple conduction paths through or around a given particle, as would occur in a physical SOFC interface due to the necking that occurs between

Downloaded From: http://fuelcellscience.asmedigitalcollection.asme.org/ on 02/06/2015 Terms of Use: http://asme.org/terms

particles during the manufacturing process. Once the conduction pathway networks were established for a given TPB, the electronic and ionic paths were each reduced to a single conduction element, following the scheme described by Fogelholm et al. [23–25]. In short, the process iteratively simplifies the conduction network by making the following reduction at each conducting node:

If node A_0 is connected to nodes $A_1, A_2, \ldots, A_n$, by conducting paths $\sigma_1, \sigma_2, \ldots, \sigma_n$,

- remove the node A_0 along with conductances $\sigma_1, \sigma_2, \ldots, \sigma_n$,
- Insert conductances

$$\sigma_{ij} = \frac{\sigma_i \sigma_j}{\sum_{1}^{n} \sigma_k} \tag{1}$$

between every pair of nodes A_i and A_j.

This iterative process was then repeated for every active TPB in the electrode, including surface exchange and transport-enabled TPBs when applicable. The electronic and ionic conduction paths were then assumed to act in series with one another. Moreover, all TPBs were assumed to act in parallel together. Therefore, given that the calculation was made in terms of conductance rather than resistance, the overall conductance for the entire electrode and a given TPB were then calculated respectively as

$$\sigma_{\text{electrode}} = \sum \sigma_{\text{TPB}}, \text{ where } \sigma_{\text{TPB}} = \frac{\sigma_{\text{ionic}} \sigma_{\text{electronic}}}{\sigma_{\text{ionic}} + \sigma_{\text{electronic}}} \tag{2}$$

As has been discussed in Ref. [4], if one were to be interested not only in optimization of electrode composition, but calculating the actual conductivity of a given electrode, some form of charge-transfer, surface exchange and transport phenomena, and possibly even activation conduction element would have to be included in the model for an accurate calculation. However, it has been shown that for the types of calculations and comparisons made in this investigation concerning overall conductance, these elements can be omitted and still provide an accurate model for the trends in conductance as related to composition [4].

2.1 Model Execution. Unless otherwise noted, the work presented in this investigation is consistent with the previous work with respect to the choice of model execution parameters. In order to establish statistical significance and utilize appropriately sized domains, data points shown herein represent the average result of 10,000 model executions, each utilizing a separate randomized variable seed that each produced a unique instance of the electrode-electrolyte interface in the Monte Carlo model. The domain size was simulated to be a 10-by-10 square, generally of monodisperse particles in all particle types. In most cases, porosity was maintained at 30%, while the amounts of the electronic, ionic, and mixed particle phases were varied, with 5% increments in electronic and ionic particle volume fractions, and 10% increments in mixed particle type volume fractions. Data was also collected for cases both with and without surface exchange and transport enabled, in order to continue to provide insight into the significance of these processes around the TPB as well as to emphasize the operational differences that are possible between anodes and cathodes. The boundary condition at the electrolyte side was consistently maintained as a dense all-ionic surface, while the current collector side was usually maintained as the idealized case of being everywhere available to gas particles and electronic particles. Any cases that investigate different boundary conditions or deviations from these standard settings mentioned above will be indicated below. However, this base case was always utilized as the idealized case against which all other variations were to be compared. Data analysis to ensure proper model execution as well as to calculate averages and standard deviations was carried out with Microsoft EXCEL, and statistical analysis by Analysis of Variance (ANOVA) tests was completed with the use of STAT-EASE software.

Table 1 TPB counts for all size distributions and boundary conditions with surface exchange and transport enabled

	5:5 Potential	5:5 Active	1:1 Potential	1:1 Active
D1	34.4340	4.1265	29.5181	8.3292
D2	34.7785	4.1031	27.5996	8.0888
D3	33.9624	4.1133	29.0741	8.2736
D4	33.5513	4.0307	28.3201	8.1396
D5	34.4877	3.9719	30.1177	8.1052
D6	32.6135	4.1858	28.3335	8.5682
Mono	47.2759	5.3549	39.0634	9.9821

3 Results

3.1 Effects of Particle Size Distribution. The general form of the trends in TPB formation with respect to electrode composition, for the idealized monodisperse case detailed above, has been discussed [3]. However, in order to determine whether or not the monodisperse case really is the optimal randomly-mixed particle size distribution, or if particle size distribution is even a factor of importance in the formation of SOFC electrode-electrolyte interfaces, this monodisperse case was compared to the particle size distributions in Fig. 3. In addition, the 1:1 (an idealized boundary with all cells accessible to both gas and electronic conductor) and 5:5 (shown in Fig. 4) current collector boundary conditions were utilized in this investigation. These were chosen to provide both the ideal and a more realistic approximation of the expected current collector geometry given the available technology for their manufacture. Finally, the composition of the electrode was constrained only to a small range (0–25% electronic conductor volume fraction) that included the peak composition of the monodisperse case. This was done in order to account for the possibility that the optimal composition for a case with one of the mixed particle size distributions could be different from the monodisperse case.

In a 10×10 cell geometry, the potential and real TPBs, for both boundary conditions as well as both with and without surface exchange and transport phenomena included, were not generally affected by the particle size and shape distribution for the composition matching the monodisperse case's optimal TPB formation. This can be seen in the TPB counts shown in Tables 1 and 2. It should be noticed, however, that although there was very little difference between the six mixed particle size distributions, all of these distributions seemed to be significantly different from the monodisperse case. Thus, in order to resolve the discrepancy in these observations, ANOVA was utilized to determine the statistical significance of the particle size and shape distribution. The analysis was carried out with the three factors of boundary condition, surface exchange and transport, and particle size distribution included in the model. The results for both active and potential TPBs indicated that the particle size distribution was not a statistically significant factor. The analysis is shown in Table 3 for active

Table 2 TPB counts for all size distributions and boundary conditions without surface exchange and transport enabled

	5:5 Potential	5:5 Active	1:1 Potential	1:1 Active
D1	3.7286	2.8205	8.9844	8.6950
D2	3.8073	2.8651	9.0779	8.7292
D3	3.7301	2.7989	8.9125	8.6616
D4	3.7773	2.8463	9.0083	8.6913
D5	3.6143	2.7437	8.6743	8.3879
D6	3.8505	2.9030	9.2393	9.0009
Mono	4.0218	3.0138	9.5768	9.3930

Downloaded From: http://fuelcellscience.asmedigitalcollection.asme.org/ on 02/06/2015 Terms of Use: http://asme.org/terms

Table 3 ANOVA analysis of active TPB formation with size distribution included as a factor

Response 1: Average Real TPBs						
Source	Sum of Squares	df	Mean Square	*F*-value	*p*-value Prob > F	
Model	186.577	8	23.322	69.183	< 0.0001	significant
A: Boundary Condition	180.889	1	180.889	536.589	< 0.0001	significant
B: Surface Exchange and Transport Transport	2.186	1	2.186	6.483	0.0197	significant
C: Size Distribution	3.502	6	0.584	1.732	0.1680	not significant
Residual	6.405	19	0.337			

TPBs; analysis of potential TPBs revealed similar results, except that boundary condition also was not significant, as expected for potential TPBs.

The hypothesis that comparison of all size distributions at a composition with 15% electronic conductor may not be an equivalent comparison between all cases was then tested by varying the composition to find the optimal composition for each individual size distribution for just the 5:5 boundary condition with surface exchange and transport enabled. The results are shown in Table 4. Again, it is clear that peak active TPBs, and even the optimal composition, did not vary amongst the particle size distributions considered, but the values for these mixed distributions were slightly different from the monodisperse case. These results, which all seem to indicate that particle size distribution is an insignificant factor in the range considered, are at odds with some of the previously reported empirical findings. Although there is not a consensus on the optimal particle size distribution, the literature typically reports that there is at least some dependence on this factor. To make sure that this result is not limited by the domain size used in the current analyses, the simulations were run on a 20-by-20 domain, with extended boundary conditions. Note that sensitivity analyses previously determined that the 10 by 10 domain was sufficiently large for the monodisperse case [3].

Only the 5:5 boundary condition was investigated, but simulations were carried out both with and without surface exchange and transport enabled for this situation. The potential and active TPB counts for these cases are presented in Table 5. At first inspection, the results mirror those found for the 10-by-10 domain case, with very little difference discernable in TPB counts amongst the size distributions considered but with a somewhat marked drop from the monodisperse case to any of the mixed particle size cases. ANOVA was then carried out on this data to ensure the validity of this conclusion. The conclusions mentioned before were again found to be correct; particle size distribution was not shown to be a significant factor in the formation of potential or active TPBs in this investigation, with a *p*-value of 0.8203 for potential TPBs, and a *p*-value of 0.9810 for active TPBs. However, TPB counts did seem to be highest when there was no particle size distribution at all, i.e., the monodisperse case. This conclusion seemingly supports the work of Sasaki et al. who reported improved performance with a narrow size distribution, as opposed to investigators such as van Heuveln et al. and Ostergard et al. who suggest a wide or bimodal particle size distribution, respectively.

Table 4 Peak active TPBs for all boundary conditions and corresponding electronic volume fraction at peak

	Peak Active TPBs	Electronic Volume %
D1	4.4305	5
D2	4.4351	0
D3	4.4723	5
D4	4.4434	5
D5	4.3553	5
D6	4.5542	5
Mono	5.3549	15

It is also interesting to note that Sasaki et al. reported a preference for not only a narrow size distribution but also for particles that are as fine as possible. This has been reflected in the results presented. The active TPB counts for the case with the 100-cell domain are lower than the active TPB counts for the 400-cell domain, with a factor of approximately two difference between these cases. Since the particle size definitions remained constant between these two cases and the current collector boundary was scaled accordingly, the 400-cell domain can be viewed as having overall finer particles than the 100-cell domain. Therefore, this second observation of Sasaki et al. was also verified by the results of this work.

3.2 Effects of Electronic:Ionic Conduction Phase Contrast. In a previous study [4], it was noted that the phase contrast, or the ratio of the electronic to ionic conductivity, of the materials chosen for the construction of a composite SOFC electrode plays a vital role in the behavior of the overall electrode conductivity as a function of electrode composition. In particular, it was noted that this trend was governed by a competition between the effects of the phase contrast and the trends in TPB formation, as a given electrode composition can not only alter the number of TPBs formed but also their most likely locations, thereby altering the lengths and relative contributions of the electronic and ionic conduction paths. Therefore, it is useful to investigate the full effects of the phase contrast on the overall electrode conductivity in order to understand the balance amongst the effects noted in the previous study.

In order to carry out this portion of the investigation, the simulation model was run with the 5:5 boundary condition, with surface exchange and transport enabled, and with a constant 30% porosity. The relative values of the conductivities were then altered in order to compute conductivities for cases with different phase contrasts. The settings for these phase contrasts are as listed in Table 6. It should be noted that the 20,000:1 phase contrast matches that previously investigated as representative of a Ni-YSZ electrode [1,4]. It should also be understood that the phase contrast values utilized were not necessarily chosen to mimic existing material sets, but rather to have a useful range of values to adequately characterize the impacts of this parameter.

Table 5 TPB counts for size distributions with an expanded, 20-by-20 cell domain

	With Sorbate Transport		Without Sorbate Transport	
	Potential	Active	Potential	Active
D1	127.41	8.6103	79.637	4.7892
D2	135.44	9.0026	87.104	4.9827
D3	127.82	8.7284	76.727	4.7088
D4	131.91	8.7389	81.006	4.8058
D5	136.30	8.4464	84.140	4.6126
D6	119.72	8.8324	72.816	5.0149
Mono	181.92	11.5780	117.16	6.2312

Downloaded From: http://fuelcellscience.asmedigitalcollection.asme.org/ on 02/06/2015 Terms of Use: http://asme.org/terms

Table 6 Electronic and ionic conductivity settings utilized to investigate phase contrast

Contrast	Electronic	Ionic
20000:1	1	5.00–05
4000:1	80	0.02
40:1	8	0.2
1:1	80	80
0.4:1	0.8	2

Full trends for the conductivity and conductivity per TPB for each of these cases were obtained. Figure 5 presents the full electrode conductivities, each of which is normalized to its own maximum value. It should be noted that each data point is actually an average, with a corresponding standard deviation; for clarity, the standard deviations have been omitted from this figure. Under a logarithmic data transformation, ANOVA provides a p-value of 0.0002 for the dependence of the normalized conductivity on the phase contrast, thereby indicating that the conductivity is strongly dependent upon this factor.

It should be noted from Fig. 5 that there are two distinct cases of optimal electrode composition: when the phase contrast was less than 40:1, the all-ionic electrode is the preferred design; for compositions with phase contrast higher than this, the all-electronic electrode is the most favorable. The fact that the 40:1 phase contrast case appears to be the composition at which the switch from one case to the next appears to occur is indicative of the percolation considerations previously reported with this model. For an electrode with percolation physics where the electronic and ionic phases are able to equivalently form percolating paths (e.g., the models defined by Sunde and others [1,2] that assume the presence of gas throughout the entire electrode and only percolate ionic and electronic phases), then there would be some electrode composition at which the path lengths are equivalent. In this case, a phase contrast of 1:1 would be the dividing phase contrast between those cases where the all-electronic case and the all-ionic case is preferable. For phase contrasts larger than 1:1, the all-electronic case would be favorable, and the all-ionic case would be preferred for smaller phase contrasts because the relative lengths of each conducting material's paths would not be a factor.

However, it has been noted several times [3,4] that the electronic phase is much less effective at percolating through the electrode when the gaseous phase is required to percolate as well, and therefore can be expected to have shorter path lengths than the ionic paths for a given electrode composition. Therefore, the longer ionic paths would have a greater effect on decreasing the overall electrode conductivity and be more detrimental to conductivity than in the balanced percolation case mentioned above. This would therefore require that the electronic phase would have to be more conductive in order to provide the same conductivity at a

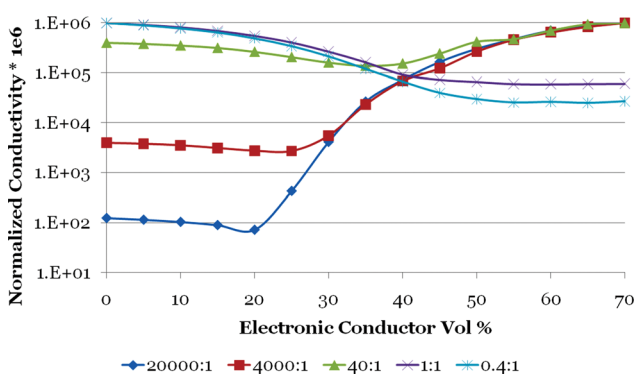

Fig. 5 Normalized overall electrode conductivity trends for all phase contrasts studied

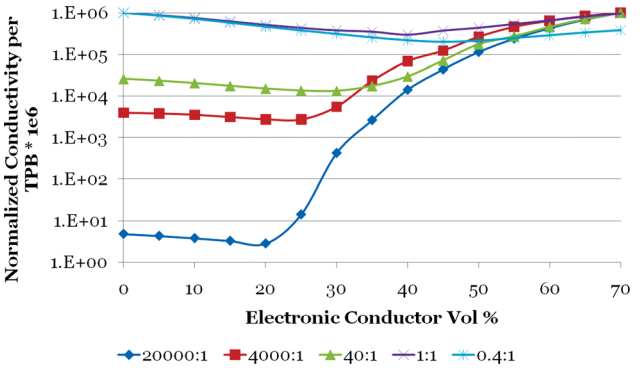

Fig. 6 Normalized individual TPB conductivity trends for all phase contrasts studied

given composition as an electrode with equivalent ionic and electronic phase percolation characteristics. Therefore, one would no longer expect that the dividing phase contrast between ionically preferred and electronically preferred electrode compositions would occur at the 1:1 phase contrast case. As observed, this dividing case would need to have a higher electronic conductivity; according to the data collected for this investigation, the electronic conductivity would have to be more than 40 times as high as the ionic conductivity in order for their percolation physics to be balanced out by their differences in conductivity. Electrodes made of materials with this particular phase contrast would then have performance characteristics nearly independent of composition. In addition, due to the dual gas-electronic boundary, the ionic phase can then be expected to have more successful interconnectivity between TPBs and the electrolyte boundary than the interconnectivity from the electronic phase to the current collector boundary. This increased interconnectivity provides improved conductivity by supplying more conducting pathways and outlets to the electrolyte for the ionic phase. Therefore, the conductivity of the ionic phase does not need to be equivalent to the electronic phase in order for the all-ionic case to be preferable, allowing the phase contrast to be greater than 1:1 for development of equivalent electronic and ionic portions of the conducting network.

The trends for the conductivity per TPB are presented in Fig. 6. It should first be noted that for certain cases, the conductivity per TPB is higher than for the total electrode. This is due to the fact that, in the conductivity per TPB data, all cases that did not include any TPBs were not included in the average calculation. This was done in order to avoid artificially skewing the results towards low conductivities. However, for the full electrode conductivity, it was deemed reasonable and accurate to include the electrodes with zero TPBs, indicative of a nonconducting portion of an electrode. In this data, it is seen that the effect of electrode composition was actually minimized at low phase contrast, and that indeed, the 1:1 phase contrast seems to indicate an electrode for which the all-electronic and all-ionic cases have equivalent conductivity. This is again as expected, since the conductivity per TPB contains less information about the interconnectivity between TPBs, thereby reducing the differences in percolation effects between electronic and ionic phases. Thus, it was shown through these two measures that the total electrode conductivity is not only dependent upon the conductivity attributed to individual TPBs, but also upon the number of TPBs and interconnectivity of the conducting phases, as expected from the dependence of TPB formation on percolation characteristics and differing percolation amongst phases.

3.3 Effects of Including Small Amounts of MEIC. It has been noted that the percolation characteristics of the SOFC electrode are particularly limited, especially for the electronic phase that must percolate all the way through the electrode to the current

Downloaded From: http://fuelcellscience.asmedigitalcollection.asme.org/ on 02/06/2015 Terms of Use: http://asme.org/terms

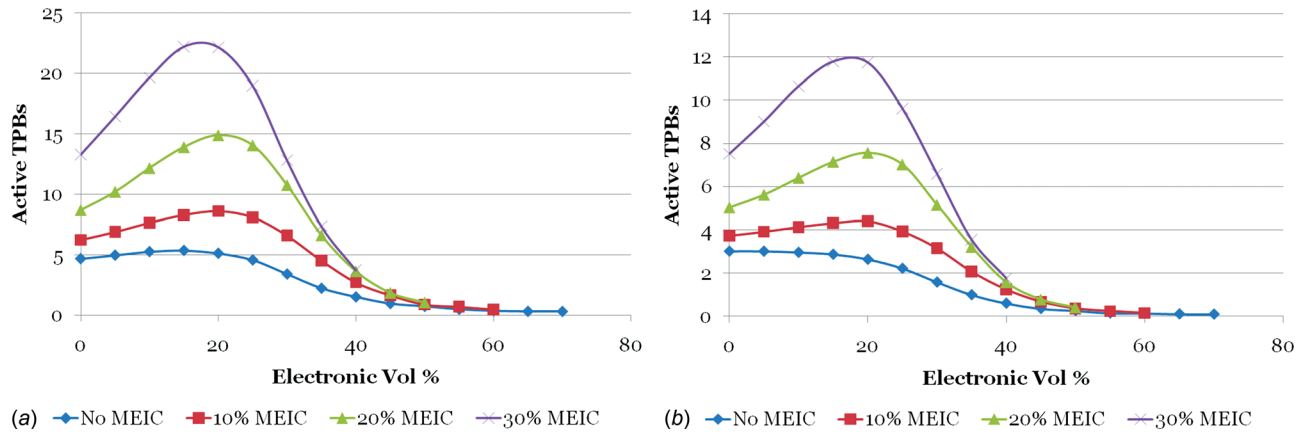

Fig. 7 Active TPB trends for various amounts of MEIC in composition of electrodes (*a*) with and (*b*) without surface exchange and transport phenomena enabled

collector, which is an especially long distance for anode-supported SOFC. Thus, it was desirable to understand how to improve the percolation of the conducting phases without hindering the percolation of the gas phase, which was itself just as limited as the electronic phase. The use of an MEIC is one effective method of doing this, and has been studied by researchers in the past. Therefore, it was of interest to understand how inclusion of this type of material in the electrode structure can improve TPB formation, and to what extent this improvement can be made. Electrode-electrolyte interfaces were therefore simulated with an MEIC constituting 10, 20, and 30% of the overall electrode composition. Porosity was held to 30%, and the 5:5 boundary condition was applied at the current collector, with the electronic and ionic phases comprising the remainder of the electrode.

The inclusion of the MEIC was found to have little effect on the shape of the potential TPB curve (though the actual number of potential TPBs increased with increasing MEIC volume fraction). However, the inclusion of increasing amounts of MEIC tended to increase not only the magnitude of the entire active TPB curve, but also to make the peak more pronounced and to slightly shift the composition of the peak. With respect to the active/potential TPB curve, the shape of the curve was highly dependent upon the amount of MEIC, exhibiting a transition from the constantly decreasing trend when no MEIC is included [3], through the development of curves with only a maximum, towards a curve with multiple local extrema, as in the 100% MEIC case studied inRef. [3]. Figure 7 displays the active TPB trends for all the amounts of MEIC studied, and the increase in active TPB counts, especially at the peak, is clear. Least-squares regression of the dependence of peak active TPB count on MEIC volume fraction revealed a quadratic relationship with a nearly 0.999 coefficient of correlation for both the case with and without surface exchange and transport phenomena. These trends are shown in Fig. 8. Thus, the trend was clearly supported by the regression; nonetheless, ANOVA was utilized once again to ensure the significance of this effect.

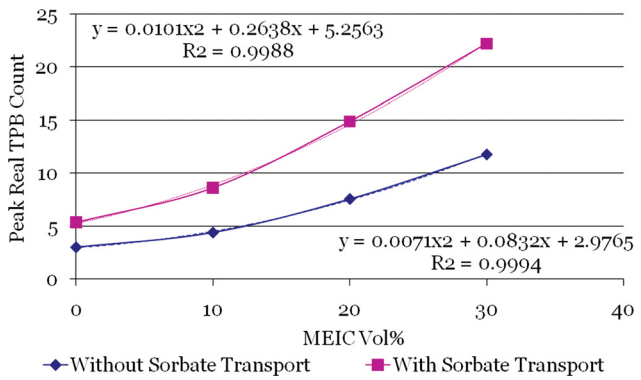

Fig. 8 Trends and correlation between peak active TPB count and MEIC volume fraction

As shown in Tables 7 and 8, the active TPB count, at any electrode composition, was found to be significantly dependent upon the MEIC content, both with and without surface exchange and transport considerations. Therefore, it is concluded that the MEIC is able to positively and significantly impact the percolation of the electronic phase, resulting in improved performance with increasing amounts of MEIC. Of course, this is true in the case that the electrode is still a composite. Previous results indicated a clearly optimized composition (volume fraction of MEIC) for an electrode that is not a composite electrode, but rather completely comprised of a porous MEIC structure. The MEIC values utilized in the current study did not indicate that the limit of the benefit with increasing MEIC content was one of the compositions studied. However, it is not expected that such a limit exists for a composite electrode where the porosity is maintained a constant, as only the solid phase particles are affected by the inclusion of the MEIC, and the MEIC serves to support the percolation properties of both phases, even though it seems to support the electronic phase more. Thus, any further investigation of electrodes with a constant porosity are expected to demonstrate that increasing MEIC content always increases TPB count.

3.4 Effects of Porosity. In all the previously reported work related to the use of this simulation model, the porosity of the simulated electrodes has been maintained at 30%. This porosity was chosen based upon a review of assumptions in previous models as well as the porosities of manufactured electrodes reported in the literature. However, in previous work with this model, it was noted that porosity can and should have an effect on TPB counts, both potential and active [3]. Therefore, it was of interest to investigate how the porosity of the electrode could alter the TPB counts and the optimal composition of the remaining portion of the electrode. Therefore, the model was run with porosities set to 4, 10, 20, 30, and 40%. For all of these simulations, the electronic and ionic phases comprised the remainder of the electrode volume, and the current collector boundary condition was maintained at the 2:2 GEE case, as this provided a balanced current collector geometry while still providing some realistic expectation of the possible impact of channels in the current collector.

It was found that the porosity was able to change the character of the active TPB count and active/potential TPB curves, exhibiting higher peaks and peaks at higher electronic volume fractions

Downloaded From: http://fuelcellscience.asmedigitalcollection.asme.org/ on 02/06/2015 Terms of Use: http://asme.org/terms

Table 7 ANOVA analysis relating peak active TPB count to MEIC volume fraction with surface exchange and transport phenomena enabled

Response 1: Active TPB Count						
Transform: Square Root		Lambda: 0.5		Constant: 0		
Source	Sum of Squares	df	Mean Square	F-Value	p-value Prob > F	
Model-MEIC Vol%	23.764	3	7.921	8.414	0.0002	significant
Residual	41.426	44	0.942			
Cor Total	65.191	47				

Table 8 ANOVA analysis relating peak active TPB count to MEIC volume fraction without surface exchange and transport phenomena enabled

Response 1: Active TPB Count						
Transform: Square Root		Lambda: 0.5		Constant: 0		
Source	Sum of Squares	df	Mean Square	F-Value	p-value Prob > F	
Model-MEIC Vol%	10.569	3	3.523	4.733	0.0060	significant
Residual	32.748	44	0.744			
Cor Total	43.317	47				

with decreasing porosity, and less pronounced peaks in active TPB counts and less curvature in the active/potential TPBs with increasing porosity. The shift towards benefiting from higher electronic volume fraction with decreasing porosity predicts optimal compositions at those more closely matching what is typically reported in the literature, as opposed to the low electronic volume fraction found to be desirable in the 30% porous electrodes previously studied. The potential TPB curve was not affected in its shape, but did have different maximum values depending upon the porosity of the electrode. A summary of the trends in these measures (peak active TPBs, maximum potential TPBs, and active/potential TPBs at the peak active TPB composition) is provided in Fig. 9. It can be seen that the peak active TPB count does decrease with increasing porosity, but the difference between cases seems slight, especially compared to the clear differences exhibited by the other factors. Therefore, ANOVA was carried out for the dependence of the peak active TPBs upon the porosity of the electrode. It was found through this analysis that peak active TPBs were not significantly affected by porosity, with a p-value of 0.7376.

This conclusion does not at all obviate the importance of the gas phase in this investigation. It has already been clearly shown [3] that the gas phase, and all surface exchange and transport features pertaining to it, are vitally important to proper understanding of the likelihood of forming potential and active TPBs. Not only has it been shown to have an obvious affect through all the data that has been found to be significantly affected by surface exchange and transport, but it has also been shown to be vitally important in the percolation physics of the electrode structure, especially for the electronic phase effectiveness of percolating through the electrode. Furthermore, investigations of the role of TPB formation in overall electrode conductivity [4] have further supported the necessity of utilizing this feature in order to properly model the ways in which the electrode microstructure can affect the overall performance.

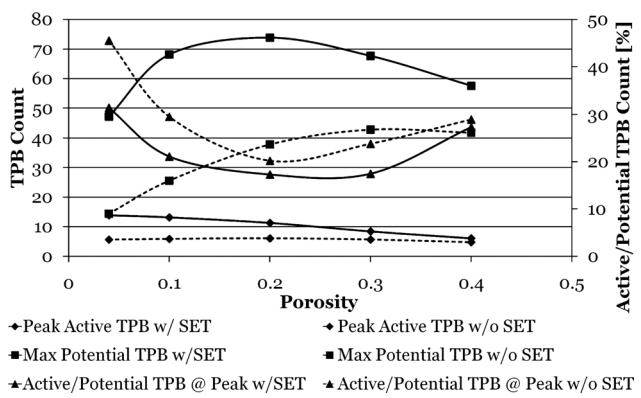

Fig. 9 Dependence of TPB formation results on porosity of electrode (SET = surface exchange and transport)

4 Conclusions

The Monte Carlo model previously utilized by the investigators to understand the fundamentals of percolation effects in the formation of TPBs and overall conductivity in SOFC electrodes has been utilized to study effects of particle properties. This investigation presents the property-function connection as it relates to the materials and operation of an SOFC electrode-electrolyte interface. This has been motivated both by the desire to provide new insight into the previous model results that did not include consideration of the percolation of the gaseous phase as well as to investigate some inconsistencies found in previously reported experimental work.

Current results confirmed the importance of considering the gaseous phase as a percolating phase in these models. Studies of the phase contrast have shown that the disparity between the percolation effectiveness of the electronic and ionic phases, which has previously been shown to be due to the inclusion of the gaseous phase, can significantly alter the expected performance and optimal composition of the electrode, depending upon the individual material conductivities. In addition, the inclusion of an MEIC in the electrode composition has been shown to significantly improve the formation of active TPBs, as one would expect from the reports of previous work. The correlation between MEIC content and optimal active TPB formation has been quantified for small amounts of MEIC volume fraction.

Downloaded From: http://fuelcellscience.asmedigitalcollection.asme.org/ on 02/06/2015 Terms of Use: http://asme.org/terms

Surprisingly, the porosity of the electrode within the range of 2–40% has not been found to be a significant factor in the amount of active TPBs formed. However, this result should not be taken to indicate that the gaseous phase does not need to be considered in studies of this type. Multiple effects of the gaseous phase and significant dependence upon its action have been repeatedly demonstrated herein and in previous works [3,4]. The importance of surface exchange and transport mechanics alone, which has been previously reported as vital to the electrochemistry of the SOFC electrode [22], requires the inclusion of these physics in fully developed and successful models of these devices.

Finally, this work has considered the disagreement in previous experimental results concerning the optimal particle size distribution. This model has confirmed the result reported by Sasaki et al. [18], finding that a narrow particle size distribution, and in particular a monodisperse size distribution, is best. Sasaki et al. had pointed to not only desiring this narrow distribution but also to utilizing particles that are as fine as possible. Through the comparison of different domain sizes, with consistent particle size definitions, this work has also verified this observation. Consideration of the results presented herein, along with the understanding previously developed with this model, can therefore aide in guiding SOFC design and construction, for both theoretical and practical applications.

Acknowledgment

This material is based upon work supported under a National Science Foundation Graduate Research Fellowship. Any opinions, findings, conclusions, or recommendations expressed in this publication are those of the author and do not necessarily reflect the views of the National Science Foundation.

References

[1] Sunde, S., 1995, "Calculation of Conductivity and Polarization Resistance of Composite SOFC Electrodes From Random Resistor Networks," J. Electrochem. Soc., **142**, pp. L50–L52.

[2] Costamagna, P., Costa, P., and Antonucci, V., 1998, "Micro-Modeling of Solid Oxide Fuel Cell Electrodes," Electrochim. Acta, **43**, pp. 375–394.

[3] Martinez, A., and Brouwer, J., 2008, "Percolation Modeling Investigation of TPB Formation in a Solid Oxide Fuel Cell Electrode-Electrolyte Interface," Electrochim. Acta, **53**(10), pp. 3597–3609.

[4] Martinez, A., and Brouwer, J., 2010, "Modeling and Comparison to Literature Data of Composite Solid Oxide Fuel Cell Electrode-Electrolyte Interface Conductivity," J. Power Sources (in press).

[5] Schneider, L. C. R., Martin, C. L., Bultel, Y., Dessemeond, L., and Bouvard, D., 2007, "Percolation Effects In Functionally Graded SOFC Electrodes," Electrochim. Acta, **52**, pp. 3190–3198.

[6] Deseure, J., Bultel, Y., Dessemond, L., and Siebert, E., 2005, "Theoretical Optimisation of a SOFC Composite Cathode," Electrochim. Acta, **50**, pp. 2037–2046.

[7] Sunde, S., 1996, "Monte Carlo Simulations of Polarization Resistance of Composite Electrodes for Solid Oxide Fuel Cells," J. Electrochem. Soc., **143**, pp. 1930–1939.

[8] Virkar, A. V., Chen, J., Tanner, C.W., and Kim, J.-W., 2000, "The Role of Electrode Microstructure on Activation and Concentration Polarizations in Solid Oxide Fuel Cells," Solid State Ionics, **131**, pp. 189–198.

[9] Tietz, F., Buchkremer, H.-P., and Stover, D., 2002, "Components Manufacturing for Solid Oxide Fuel Cells," Solid State Ionics, pp. 152–153, 373–381.

[10] Savignat, S. B., Chiron, M., and Barthet, C., 2007, "Tape Casting of New Electrolyte and Anode Materials for SOFCs Operated at Intermediate Temperature," J. Eur. Ceram. Soc., **27**, pp. 673–678.

[11] Li, C.-J., Li, C.-X., and Wang, M., 2005, "Effect of Spray Parameters on the Electrical Conductivity of Plasma-Sprayed $La_{1-x}Sr_xMnO_3$ Coating for the Cathode of SOFCs," Surf. Coat. Technol., **198**, pp. 278–282.

[12] Ge, X., Huang, X., Zhang, Y., Lu, Z., Xu, J., Chen, K., Dong, D., Liu, Z., Miao, J., and Su, W., 2006, "Screen-Printed Thin YSZ Films Used as Electrolytes for Solid Oxide Fuel Cells," J. Power Sources, **159**, pp. 1048–1050.

[13] Zheng, R., Zhou, X. M., Wang, S. R., Wen, T.-L., and Ding, C. X., 2004, "A Study of Ni+8YSZ/8YSZ/$La_{0.6}Sr_{0.4}CoO_{3-\delta}$ ITSOFC Fabricated by Atmospheric Plasma Spraying," J. Power Sources, **140**, pp. 217–225.

[14] van Dieten, V. E. J., and Schoonman, J., 1991, "Thin Film Techniques for Solid Oxide Fuel Cells," Solid State Ionics, **57**, pp. 141–145.

[15] Wang, H. B., Song, H. Z., Xia, C. R., Peng, D. K., and Meng, G. Y., 2000, "Aerosol-Assisted MOCVD Deposition of YDC Thin Films on (NiO+YDC) Substrates," Mater. Res. Bull., **35**, pp. 2363–2370.

[16] Meng, G., Song, H., Dong, Q., and Peng, D., 2004, "Application of Novel Aerosol-Assisted Chemical Vapor Deposition Techniques for SOFC Thin Films," Solid State Ionics, **175**, pp. 29–34.

[17] Juhl, M., Primdahl, S., Manon, C., and Mogensen, M., 1996, "Performance/Structure Correlation for Composite SOFC Cathodes," J. Power Sources, **61**, pp. 173–181.

[18] Sasaki, K., Wurth, J. P., Gschwend, R., Godickemeier, M., and Gauckler, L. J., "Microstructure-Property Relations of Solid Oxide Fuel Cell Cathodes and Current Collectors," J. Electroch. Soc., **143**, pp. 530–543 (1996).

[19] van Heuveln, F. H., Vanberkel, F. P. F., and Huijsmans, I. P. P., 1993, "Characterization of Solid Oxide Fuel-Cell Electrodes by Impedance Spectroscopy and IV-Characteristics," *High Temperature Electrochemical Behavior of Fast Ion and Mixed Conductors, Proceedings of the 14th Risø International Symposium on Material Science*, F. W. Poulsen, J. J. Bentzen, T. Jacobsen, T. Skou, and M. J. L. Østergård, eds., RISØ, Roskilde, p. 53.

[20] Dusastre, V., and Kilner, J. A., 1999, "Optimisation of Composite Cathodes for Intermediate Temperature SOFC Applications," Solid State Ionics, **126**, pp. 163–174.

[21] Ostergard, M. J. L., Clausen, C., Bagger, C., and Mogensen, M., 1995, "Manganite-Zirconia Composite Cathodes for SOFC: Influence of Structure and Composition," Electrochim. Acta, **40**, pp. 1971–1981.

[22] Adler, S.B., 2004, "Factors Governing Oxygen Reduction in Solid Oxide Fuel Cell Cathodes," Chem. Rev., **104**, pp. 4791–4843.

[23] Fogelholm, R., 1980, "The Conductivity of Large Percolation Network Samples," J. Phys. C, **13**, pp. L571–L574.

[24] Fogelholm, R., 1980, *An Elimination Method for the Conductance of Percolation Networks*, Stockholm, Royal Institute of Technology.

[25] Fogelholm, R., 1981, "Computation for Conductance Distributions of Percolation Lattice Cells," *Proceedings of the 1981 ACM Symposium on Symbolic and Algebraic Computation*.

Downloaded From: http://fuelcellscience.asmedigitalcollection.asme.org/ on 02/06/2015 Terms of Use: http://asme.org/terms